A Comparison of Two Non-Destructive Techniques for Determining the Modulus of Elasticity of Small-Diameter Roundwood

A Thesis
Presented in Partial Fulfillment of the Requirements for the
Degree of Master of Science
with a
Major in Natural Resources
in the
College of Graduate Studies
University of Idaho
by
Alexander D. Anderson

Major Professor: Thomas Gorman, Ph.D.
Committee Members: Armando McDonald, Ph.D.; Andrew Nelson, Ph.D.
Department Administrator: Randall Brooks, Ph.D.

May 2017

Authorization to Submit Thesis

This thesis of Alexander D. Anderson, submitted for the degree of Master of Science with a Major in Natural Resources and titled "A Comparison of Two Non-Destructive Techniques for Determining the Modulus of Elasticity of Small-Diameter Roundwood," has been reviewed in final form. Permission, as indicated by the signatures and dates below, is now granted to submit final copies to the College of Graduate Studies for approval.

Major Professor: ________________________________ Date: ____________
Thomas Gorman, Ph.D.

Committee Members: ________________________________ Date: ____________
Armando McDonald, Ph.D.

________________________________ Date: ____________
Andrew Nelson, Ph.D.

Department Administrator: ________________________________ Date: ____________
Randall Brooks, Ph.D.

Abstract

Because small-diameter trees are more important commercially than ever before, deriving the greatest value possible from those logs is necessary. In an effort to promote a simple, low-cost method for determining stiffness in small-diameter roundwood, we tested 50 logs (both 4-inch and 6-inch) of varying ages and species using two non-destructive evaluation techniques for grading logs—stress-wave velocity (in conjunction with density) to determine dynamic modulus of elasticity (MOE) and mid-point loading to measure static MOE. We also looked at a sample set of 90 lodgepole pine logs from a previous study to explore whether or not the MOE values taken at 45° increments fit a sine wave. Both SWV and mid-point loading gave us MOE results that correlated well with MOE values derived from third-point bending. The analysis of the 90-log data set showed more than half of the logs fitting a sine wave at a 95% confidence level.

Acknowledgements

I would be remiss if I did not acknowledge some of the people who played a role in the completion of this thesis. Firstly, I would like to thank Dr. Michael Wilder, from the University of Idaho’s Computer Science program, whose help was invaluable in bringing the FlexGrade machine back from the dead. Without his help, it is unlikely that this research would have been possible in its current form.

I would also like to thank Dr. Norman Pendegraft, from the University of Idaho’s College of Business and Economics. He was an invaluable resource when considering methods of tackling the different ways in which to address log orientation’s impact on MOE. In that same vein, I would like to thank the people from the Statistical Consulting Center who helped me wade through swaths of old data to analyze only the parts relevant to my project.

I would like to acknowledge Drs. Mark Kimsey, Andrew Nelson and Robert Keefe for their assistance in obtaining logs for the study. Quite literally, there would have been no study had there been no logs, so I greatly appreciate their help.

Without the guidance, knowledge, patience and perseverance of Dr. Thomas Gorman, it is doubtful that I would have been able to finish this thesis. He provided me with assistance when needed, but also granted me independence when it was helpful. His thoughtfulness when helping me select the most appropriate coursework and his interest in my success, both inside and outside the classroom, is greatly appreciated.

Finally, I must thank my wife, Whitney Anderson, whose love and support has been invaluable. She made myriad sacrifices to facilitate our life here—nearly 2,000 miles from home—and for that I’m forever grateful. She has also given me the greatest gift of all, our beautiful daughter—Paige Elizabeth Anderson.

Table of Contents

List of Tables

List of Figures

Introduction

As small-diameter trees continue to gain importance in the forest products marketplace, finding ways to utilize those logs to their full potential will become increasingly imperative. Thinning overstocked stands in the northwestern United States has become more common as many thousands of acres are overstocked, resulting in increased fire risk and suppression of tree growth. The logs that come out of these overstocked stands are almost all small-diameter logs that do not have nearly the same economic value as larger-diameter logs coming from more actively managed stands of timber [5]. That does not mean that these logs are always of inferior quality, though—much of the Douglas-fir, for example, that occurs as understory is actually quite stiff because of its suppressed growth and resultant tight growth rings. Currently, there is not a strong market demand for small-diameter logs, though it is possible that increasingly intensive plantation management on private and state lands will significantly increase the number of small-diameter logs making their way to market. Thus, uses beyond the long-time industry standard for small-diameter log use in post-and-pole mills are being considered as methods for creating value-added products from small-diameter logs, including use as roundwood trusses and in other structural applications [13].

Research geared toward determining how effectively logs can be mechanically graded to determine stiffness and strength has been ongoing since the 1990s, as it has been deemed unlikely that visual grading adequately predicts the potential load-carrying capacity of logs [8]. It is assumed that the conservative nature of *ASTM D 3957* results in logs larger in diameter being called for than are really required, which is why there has been some effort to establish mechanical grading procedures for logs intended for use in structural applications [9]. Though it is not the intent of this paper to produce a true grading system for logs, there have been other research efforts toward that end. In a similar effort to those in progress to create machine stress rating (MSR) grades for logs, an effort at creating grades for large timbers was undertaken nearly 20 years ago. As was the case for dimension lumber (and will be the case, ultimately, for logs), it was necessary to establish a relationship between modulus of rupture (MOR) and modulus of elasticity (MOE). Once that relationship is established through extensive testing, it is possible to sort timbers or logs into grades [12].

One of the results of the increase in available small-diameter logs is the specialization of certain mills in what is called ton wood—a trade term for logs too small in diameter to be utilized at a traditional sawmill. Plummer Forest Products in northern Idaho is one such mill, sawing logs with a diameter of 8” or less on the large end exclusively [14]. In order to maximize the profitability of the lumber sawn from small-diameter logs, MSR has become popular. While the machine grading of lumber originated in the 1960s, it did not become a common practice until 20-30 years ago [6]. The advantage of MSR lumber is the potential to offer a higher-value alternative over visually graded lumber, since the MSR lumber from small-diameter logs produces lumber with a lower coefficient of variation in MOE than visual grading is capable of [4,5]. Low variability in stiffness and strength allows higher design values to be assigned to lumber that has been evaluated for stiffness.

The desire to determine more precise stiffness and strength values for small-diameter logs is not solely the domain of lumber producers. There is significant interest in the use of small-diameter logs in either the debarked or doweled state for a variety of applications. There have been examples of small-diameter logs utilized as structural elements in “round-wood engineered structures” [10], such as bridges and outdoor buildings [7]. Using small-diameter logs, rather than the lumber sawn from those logs, leaves the product less susceptible to warp during drying, offers a product with lower processing costs and provides for a load carrying capacity that is two-to-four times higher than the largest rectangular member that can be cut from the log [10].

Work has already been done to demonstrate the efficacy of mechanically grading logs for structural use. As early as 2005, logs were mechanically graded for use as structural members in walking bridges [7]. Some recent research has focused on the possibility of making mechanical log grading a simpler, more accurate process that has the potential to be implemented on an industrial scale. With R^2 values ranging from 0.94 to 0.96 when evaluating the static bending MOE of a single-point bending test compared to the static bending MOE derived from a third-point bending test [2,9], it is clear that a strong relationship has been demonstrated. Furthermore, there has been investigation into whether or not stress wave velocity (SWV) can be a strong predictor of MOE. The results, when compared to the static MOE based on third-point bending results, were not as consistent as those comparing single-point to third-point bending (R^2 = 0.67) [9].

Recent research at the University of Idaho suggests that the orientation of a log when subjected to bending has an impact on the measured MOE. Also, when the MOE of a log is measured in bending at 8 points (every 45°), the MOE values appear to fit a sine wave function. Bowers [2] utilized mid-point and third-point bending to determine the MOE of 90 lodgepole pine logs at 45° intervals around their circumferences, as shown in Figure 1.

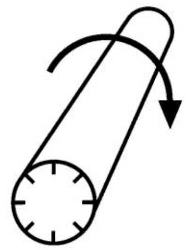

Figure 1. – Rotational pattern used during Bowers' static bending tests to measure MOE at 45° increments [2].

Though single-point loading and SWV as methods of determining MOE have been evaluated in the literature, they have never been compared to third-point bending MOE results across a variety of species with significantly disparate MOE values. The first objective of this paper is to compare the accuracy of single-point loading and SWV to third-point bending when determining the MOE of small-diameter roundwood across a wide array of MOE values and several species of wood in order to develop a simple, more economically viable test to determine log stiffness. The second objective is to explore the effects of a log's orientation during testing and investigate whether or not that orientation has a significant impact on stiffness.

Methods

We obtained 50 logs of five different species for this study and had them doweled by Camas Post Yard, a post and pole company in Craigmont, Idaho, owned by Pacific Western Lumber. Nineteen of the logs were 6 inches in diameter: 9 western larch (*Larix occidentalis*) and 10 lodgepole pine (*Pinus contorta*). The remaining 31 logs were doweled to 4 inches in diameter: 10 Douglas-fir (*Pseudotsuga menziesii*), 10 ponderosa pine (*Pinus ponderosa*), 10 grand fir (*Abies grandis*) and 1 western larch. In order to maintain a preferred span-to-depth ratio of 21:1, the 6-inch logs were cut to approximately 12-foot lengths, while the 4-inch logs were cut to 8 feet in length. Logs were allowed to air dry for several weeks in the Renewable Materials Laboratory. They were stacked in racks, and rows were separated by stickers to allow adequate ventilation. The logs were visually graded by a certified lumber grader from Timber Products Inspection, Inc., utilizing the current grading standards for roundwood [16].

We measured the diameter of each log to the nearest hundredth of an inch and their lengths to the nearest inch. Each log was also weighed, which—with the volume determinations—allowed us to accurately compute the logs' densities. Additionally, the moisture content (MC) of each log was measured with a Delmhorst RDM-3 moisture meter. It is important to note moisture content, as MOE has been demonstrated to increase by 14% or more when dried from the green state to 17.5% MC [11]. All the 6-inch logs tested fell between 13-23% MC and the 4-inch logs were all measured at 7-13% MC—all well below the fiber saturation point. We did not target a specific moisture content percentage because we were not testing the ultimate strength of each log; rather, we were simply testing the stiffness of each log at a certain point in time.

Before stiffness testing began, each log was marked to indicate a 0° and 90° orientation for bending tests. The 0° orientation was chosen arbitrarily for all the logs except for the ponderosa pine, which was composed almost entirely of juvenile wood and, therefore, had such severe warp that a desirable orientation was chosen to allow at least one accurate measurement.

After density and moisture content were determined, the stress wave velocity for each log was measured using the fibre-gen Hitman HM200, as shown in Figure 2. MOE was then calculated using this Equation (1) to determine dynamic MOE using stress-wave velocity [3]:

$$MOE_{dyn} = \rho V^2 \quad (1)$$

where:
ρ = nominal density
V = acoustic velocity

Figure 2. – One of the 6” logs is tested using the Hitman HM200 to measure stress wave velocity.

Each log underwent two tests—one at 0° and another at 90°—on the Instron 5500R in third-point loading to determine their static MOE, according to the standard provided in

ASTM D 198 – 08 [1]. We utilized a 10,000 pound load cell to measure load and a linear variable differential transducer (LVDT) to measure deflection. The test set up for these third-point loading tests is shown in Figure 3.

Figure 3. – Instron 5500R machine used for third-point testing to determine static MOE. The 6" log pictured is being tested at the 90° orientation.

Next, the logs were transferred to the FlexGrade machine, a mid-point load bending test machine fabricated by seniors in the University of Idaho mechanical engineering program and shown in Figure 4. The FlexGrade machine utilizes a hydraulic ram to apply a pre-selected mid-point load to the center of a log (which is supported at both ends) with a

2,000-pound load cell, while a Keyence IA-100 laser analog sensor—which has a margin of error of +/- 0.15% of full scale and a repeatability of 10μm—is used to measure deflection. Once load and deflection measurements are taken, the static MOE is calculated by the proprietary software using Equation (2), as provided by Wang, *et al.* [17]:

$$MOE = (PL^3)/(48\Delta I) \tag{2}$$

where:
P = load within the proportional limit
L = span
Δ = deflection at midspan within the proportional limit
I = moment of inertia

Figure 4. – FlexGrade machine used to perform mid-point testing on small-diameter logs.

In order to ensure consistent results, the MOE of all logs was determined via all three methods the same day their densities and moisture contents were calculated and measured.

We assessed whether or not MOE values determined for log positions located at opposite points, or 180° from each other, were similar for all 60 of the 4-inch logs (0° and 180°; 45° and 225°; 90° and 270°; and 135° and 315°). Because there are four unique sets of data for each log, 240 points of data were compared. We also used Bowers' entire 90-log data set to assess the theory that a sine wave function would fit the variation in MOE for each log. We performed this assessment by utilizing a non-linear least squares method in Excel to analyze all the MOE results for each of the logs in Bowers' lodgepole pine sample set. The routine to perform this analysis using Excel is described by Pieterse and Lewis [15]. The results of the least squares fit to a sine wave function for each of the 90 logs were then placed in an ANOVA table and their fit was evaluated.

Results and Discussion

The average diameter for the 6-inch logs after air drying in the laboratory drying was 5.9 inches, while the average diameter for the 4-inch logs after drying was 3.9 inches. Of the nineteen 6-inch logs, twelve met the Unsawn Round grade (the highest TPI grade allowable for a doweled log), two were graded as a No. 3 and five were determined to be "cull logs." Three of the lodgepole pine cull logs were discarded due to large knot whorls, while the other two logs were culled due to the presence of at least one knot over 3 inches in diameter.

All 10 of the ponderosa pine logs were deemed to be cull logs, which was not unexpected given that they were obtained from young trees and contained large knots. These logs averaged 11 years of age, so they were exclusively comprised of juvenile wood. Nine of the Douglas-fir logs met the Unsawn Round grade which was also anticipated, given their straight grain orientation and lack of knot whorls. The single 4-inch Douglas-fir that was graded as a No. 3 possessed excessive slope of grain (1:8). The 4-inch grand fir logs were also straight-grained and generally free of excessive knot whorls and large knots. Five of the grand fir logs met the Unsawn Round grade, while four of them were determined to meet the No. 2 log grade due to excessive slope of grain.

The solitary grand fir cull log contained a knot whorl that warranted a significant downgrade. These results are summarized in Table 1. The data shown in Table 1 indicates the number of logs by species, as well as average diameter. The table also shows the number of logs of each species given a particular grade by the TPI representative, along with the high and low range of ages of the logs from each species (along with the average age for each species).

Table 1. – Log species, diameter, grade and age.

Species	**# of Logs**	**Average Diameter (in.)**	**TPI Log Grades *(# of each grade)***	**High Ring Count Range (*Average*)**	**Low Ring Count Range (*Average*)**
Larch	9	5.9	Unsawn Round (*9*)	51-69 (*60*)	28-56 (*47*)
Larch	1	3.9	No. 1 (*1*)	10 (*10*)	6 (*6*)
Lodgepole Pine	10	5.9	Unsawn Round (*3*), No. 3 (*2*), Cull (*5*)	19-39 (*33*)	6-22 (*14*)
Ponderosa Pine	10	3.9	Cull (*10*)	10-13 (*11*)	5-9 (*6*)
Douglas-fir	10	3.9	Unsawn Round (*9*), No. 3 (*1*)	20-52 (*31*)	8-33 (*18*)
Grand Fir	10	3.9	Unsawn Round (*5*), No. 2 (*4*), Cull (*1*)	16-33 (*23*)	10-18 (*14*)

Given the variety of species and ages of the logs, it was expected that MOE values would range from very low (juvenile ponderosa pine) to very high (suppressed growth western larch). This variation was desirable because it allowed us to validate the two non-destructive techniques across a wide array of stiffness values to ensure that their accuracy was not relegated to a small range of MOE values. The graphs shown in Figures 5, 6, 7 and 8 below demonstrate the consistency of both mid-span testing to determine static MOE and SWV as a means of calculating dynamic MOE.

The MOE results shown in Figure 5 are the results of the 0° starting point for determining the MOE of each log using the FlexGrade machine to impose a mid-point load and measure deflection. The resultant MOE is compared to the MOE determined using the ASTM D-198 bending test with the log oriented in the same position.

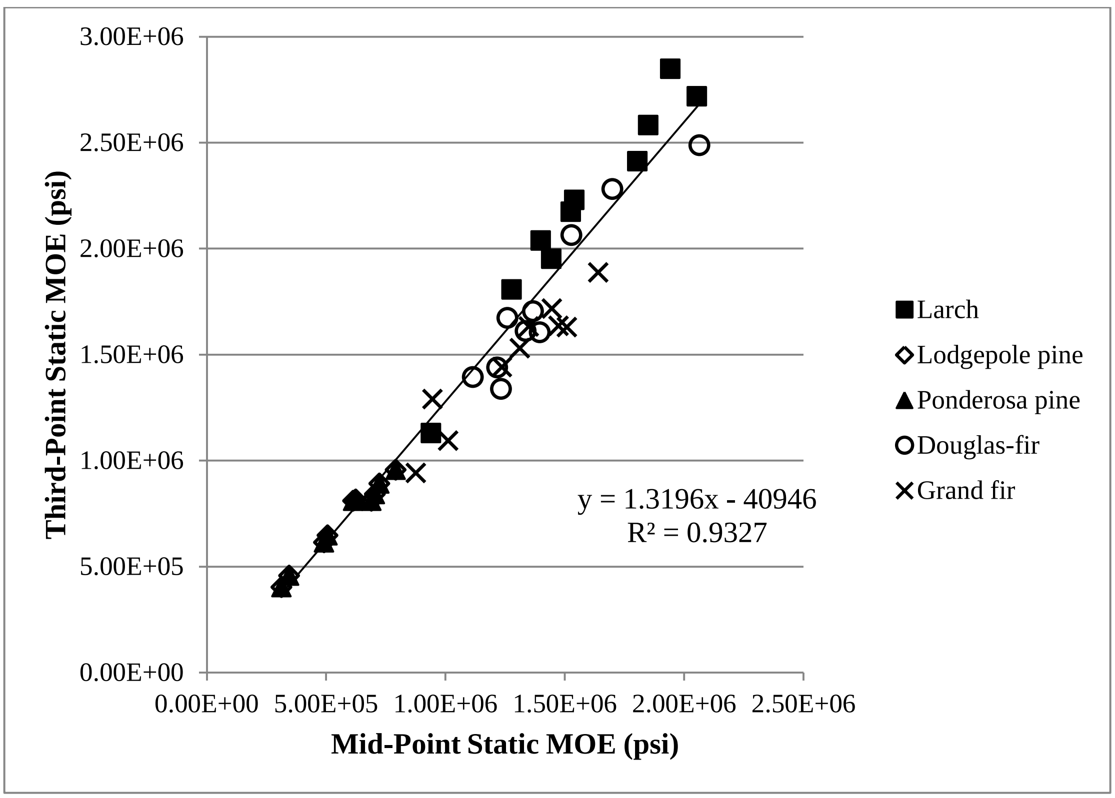

Figure 5. – Correlation between static MOE values for third-point bending and single point load tests.

The MOE of each log as determined by mid-point loading correlated very well (R^2 = 0.9327) with the MOE as determined by the ASTM D-198 bending test. This result confirms the strong correlations found in previous studies that compared mid-point loading to third-point loading. We discovered, though, that the mid-point test underestimated the static MOE as determined by the third-point bending test, but did so consistently enough to give a strong correlation. The y-intercept and slope determined from our analysis was then used to adjust calculated MOE in the software used to run the FlexGrade machine to provide static MOEs that much more closely replicated the results from the third-point bending tests.

The correlation between MOE determined via stress wave velocity and the ASTM D-198 bending tests was also quite high (R^2 = 0.9605), as seen in Figure 6. This correlation is significantly higher than that found by Green, *et al.* in an earlier study (R^2 = 0.67) [8]. The difference is likely due to the lack of individual density measurements for each log in that study. Without an accurate density, the dynamic MOE estimates will not be as accurate as they are with the correct density included in the MOE calculated using Equation 1. While the dynamic MOE figures were not as low as the results from the mid-point bending test, the dynamic MOE results were lower than the static MOE as defined by third-point bending for almost every log.

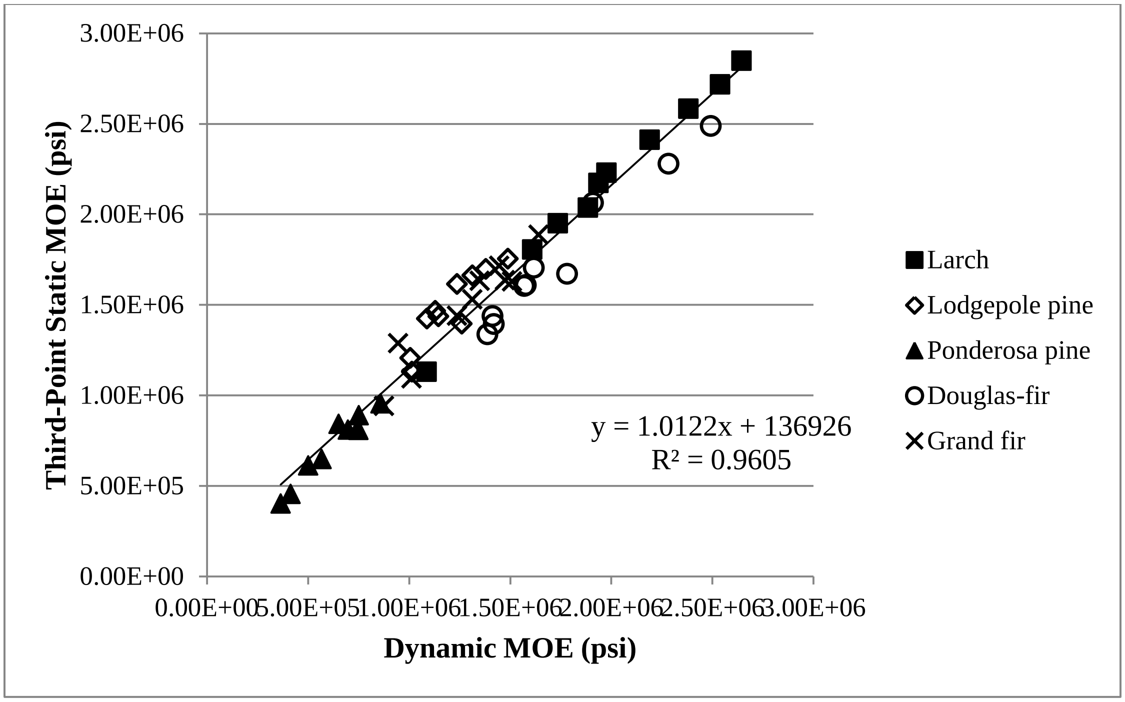

Figure 6. – Correlation between baseline static MOE values for third-point bending and SWV.

The comparison shown in Figure 7 is the product of measuring the MOE values at both orientations (0° and 90°) and utilizing the average of those values.

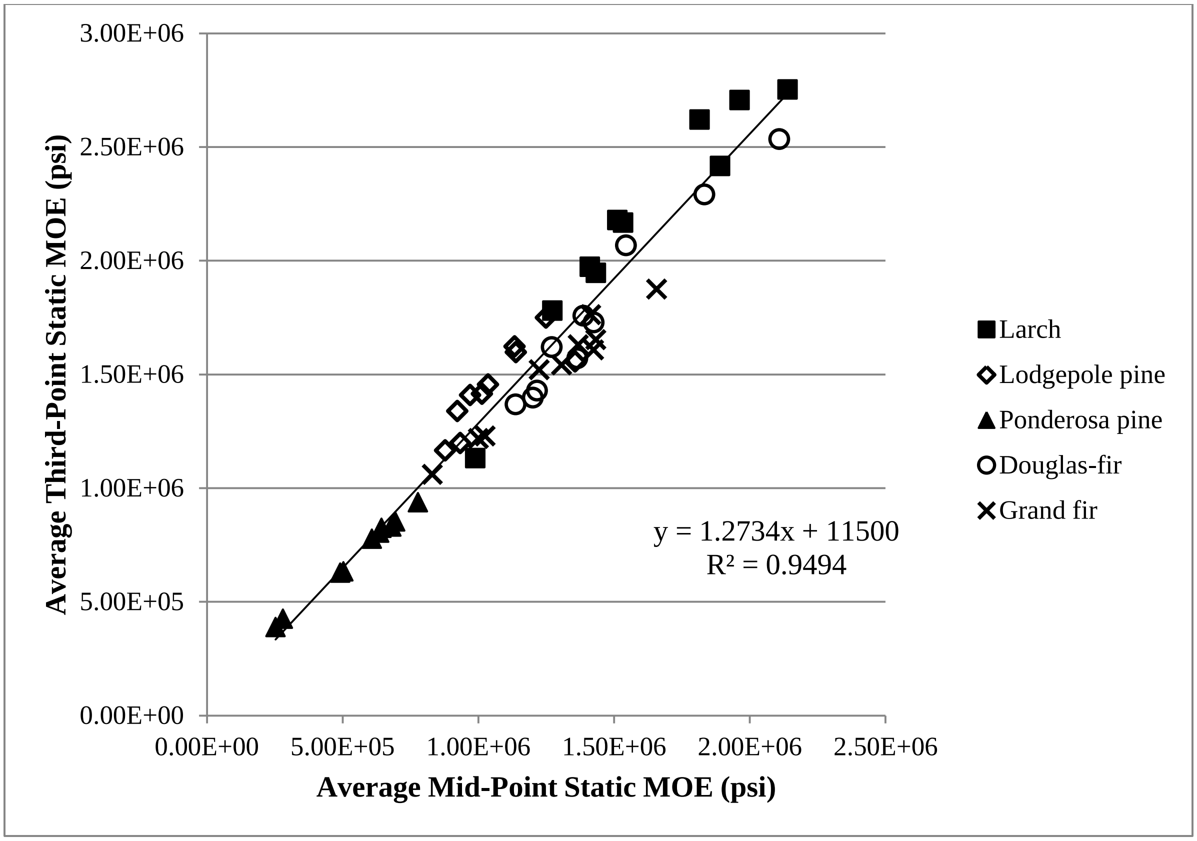

Figure 7. – A comparison of the average static MOE values measured by both third-point and mid-point.

The results here indicate that using the average of two measurements for each log resulted in an r-squared value that is very slightly higher than using only a single measurement for each log (R^2 = 0.9494 vs. R^2 = 0.9327, respectively). The difference in r-squared values is possibly attributable to an increase in accuracy, due to the use of two measurements for each bending test; however, the results are so similar that it could also be attributable to “noise” in the testing itself or simply a result of the variability within wood. To properly assess these results, further testing on a larger scale is necessary.

When comparing the average MOE of each log in third-point bending to the dynamic MOE of each log, the correlation is slightly lower than the correlation when comparing the single, initial third-point MOE value for each log to the dynamic MOE (R^2 = 0.9550 vs. R^2 =

0.9605, respectively). We anticipated at least a slight increase in the correlation between the static and dynamic MOE values when using the average third-point static MOE, as was evidenced in the third-point and mid-point MOE comparison, so this result was unexpected. The difference between the correlation values is so minor (< 0.01) that it is not necessarily meaningful to suggest that either correlation is stronger or weaker than the other.

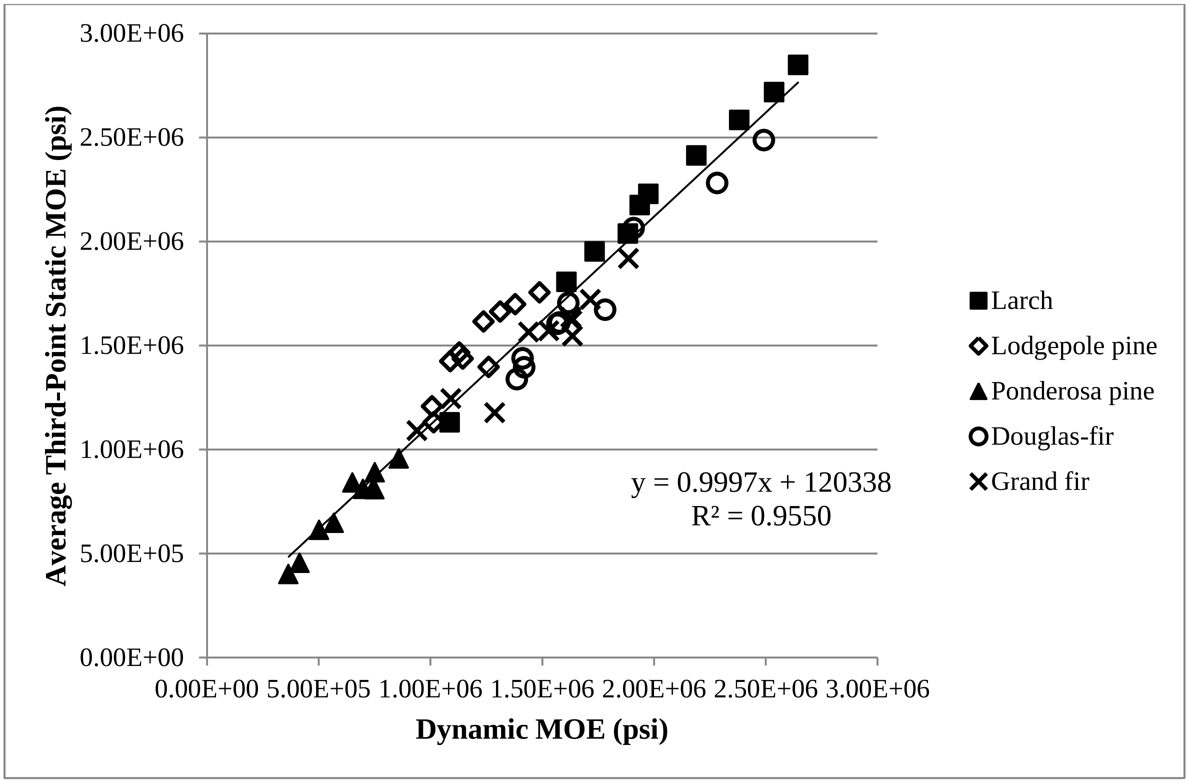

Figure 8. – A comparison of the dynamic MOE values and average third-point static MOE values.

As can be seen in the preceding graphs (Figures 5,6,7 and 8), the western larch logs were, generally, the stiffest and the ponderosa pine logs were the least stiff. The lodgepole pine logs fell near the middle in terms of MOE values. With the exception of the mid-point static MOE values in Figure 5 (which were lower than in any other comparison), the grand fir logs were also, in general, near the middle of the MOE values for the data set. The species with the greatest diversity of MOE values was Douglas-fir, which ranged from about 1.4 x 10^6 psi to 2.5 x 10^6 psi, according to the results from the third-point static bending test. This variability is likely due to the wide variety of ages present in the Douglas-fir. The oldest wood present ranged from 20-52 years old, while the youngest wood present ranged from 8-33 years old. This range suggests that some of the logs were more than half a century old, suppressed growth trees, while others were young, fast-growing trees with juvenile wood present on their outer surface.

When comparing the MOE results measured non-destructively to the MOE values assigned to each TPI grade, there are significant differences. Western larch, for example, has an MOE of only 1.6 x 10^6 psi when graded as Unsawn Round by TPI; however, we measured several western larch logs in third-point bending that produced MOE results above 2.0 x 10^6, with some as high as 2.8 x 10^6. The grand fir and lodgepole pine logs were given a variety of visual grades, which makes sense given their wider distribution along the middle third of the MOE range present in the data set. All of these results confirm the value of non-destructive evaluation, since many of the logs were deemed to be significantly stiffer than the visual grade alone would have warranted.

When examining the potential sine wave fit from the data in the same study by Bowers, the ANOVA results indicated that 55 of the 90 lodgepole pine logs, or 61%, had a confidence level of at least 95%, which demonstrates a strong relationship between the eight static MOE values for those logs and a sine wave. Furthermore, 68% of all the logs show a confidence level of at least 90%, 79% show a confidence level of at least 75%, and 91% of all the lodgepole pine logs in Bowers' data set show a confidence interval of at least 50%.

Figure 9 shows all 90 logs in a distribution by confidence level. There were only nine logs showing less than 50% confidence that the data fits a sine wave function, while 61 showed a confidence level of 90% or greater.

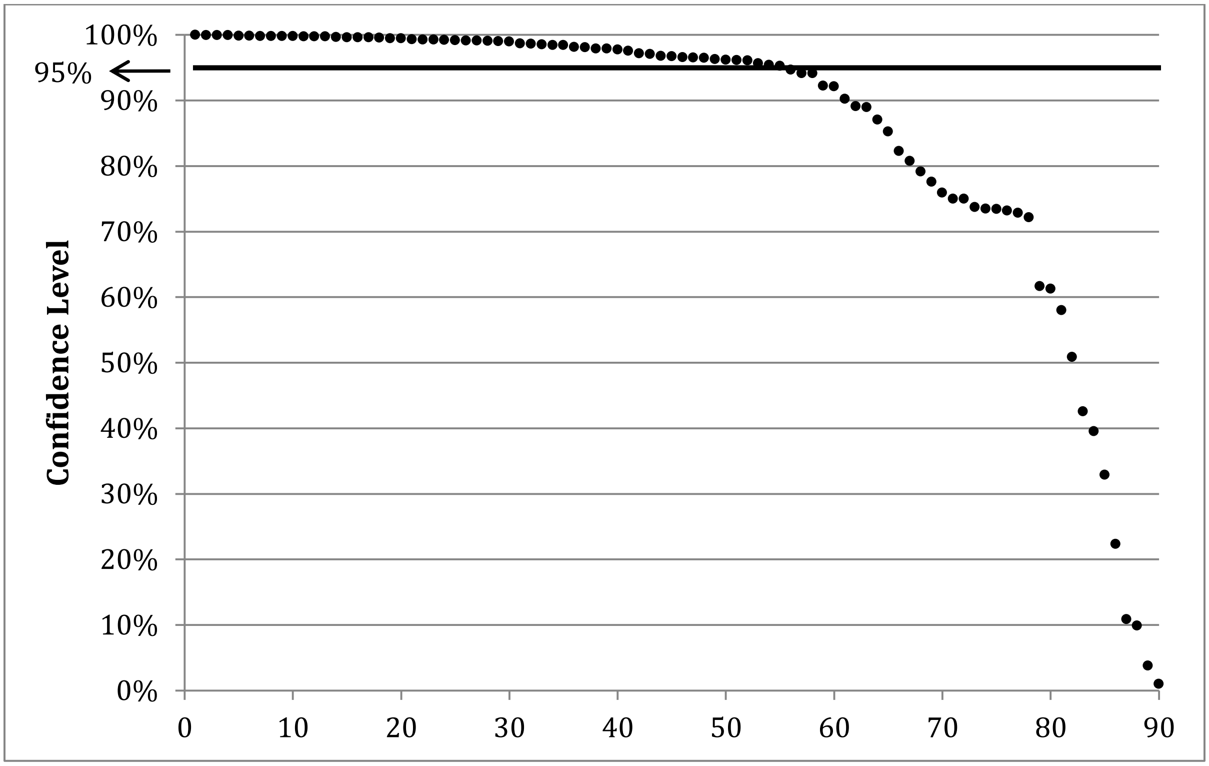

Figure 9. – Confidence level of sine wave fit for Bowers' 90-log lodgepole pine data set.

Conclusion

- The FlexGrade machine (mid-point test) provided MOE results that correlate well with the MOE determined using the ASTM third-point bending method for determining stiffness (R^2 = 0.9327).
- The dynamic MOE of each log—determined by stress-wave velocity and density—also correlated well (R^2 = 0.9605) with the average third-point loading bending test MOE value. This method—if used in conjunction with density data for each log—shows the greatest potential for a quick, inexpensive method for determining log stiffness.
- Taking two MOE measurements—with the second measurement taken when the log is rotated by 90°—and averaging the results of those MOE values provided only a slightly better correlation than using a single MOE value when comparing static MOEs (R^2 = 0.9494 vs. R^2 = 0.9327, respectively).
- Taking two MOE measurements—with the second measurement taken when the log is rotated by 90°—and averaging the results of the static MOE values provided a nearly identical correlation to using a single MOE value when comparing static MOE to dynamic MOE (R^2 = 0.9550 vs. R^2 = 0.9605, respectively).
- Using data from a previous study of 90 lodgepole pine logs, we found that a non-linear least squares analysis of the data set indicated that 61% of the measurements fit a sine wave at a 95% confidence level. We also found that 79% of logs fit a sine wave when the confidence level was reduced to 75%.

References

[1] American Society for Testing and Materials. 2015. Standard Test Methods of Static Tests of Lumber in Structural Sizes. ASTM D 198-15. Annual Book of Standards, Vol. 04.10. ASTM, West Conshohocken, Pa.

[2] Bowers, C. L. 2012. *Use of a single, mid-span load to determine the MOE of small diameter structural logs*. Master's thesis. University of Idaho, Moscow.

[3] Carter, P., Chauhan, S., and J. Walker. 2006. Sorting logs and lumber for stiffness using Director HM200. *Wood and Fiber Science*. 38(1):49-54.

[4] Erikson, R. G. 1997. Mechanical Grading Opportunities for Lumber Sawn from Small-Diameter Logs. Master's thesis. University of Idaho, Moscow.

[5] Erikson, R. G., Gorman, T. M., Green, D. W., and D. Graham. 2000. Mechanical Grading of Lumber Sawn from Small-Diameter Lodgepole Pine, Ponderosa Pine, and Grand Fir Trees from Northern Idaho. *Forest Prod. J.* 50(7/8):59-65.

[6] Galligan, W. L. and K. A. McDonald. 2000. Machine Grading of Lumber: Practical Concerns for Lumber Producers. Gen. Tech. Rept. FPL-GTR-7 (rev.). USDA Forest Serv., Forest Prod. Lab., Madison, WI. 39 pp.

[7] Green, D. W., Evans, J. W., Murphy, J. F., Hatfield, C. A., and T. M. Gorman. 2005. Mechanical Grading of 6-Inch-Diameter Lodgepole Pine Logs for the Travelers' Rest and Rattlesnake Creek Bridges. Res. Note FPL-RN-0297. USDA Forest Serv., Forest Prod. Lab., Madison, WI. 17 pp.

[8] Green, D. W., Gorman, T. M., Evans, J. W., and J. F. Murphy. 2004. Improved grading system for structural logs for log homes. *Forest Prod. J*. 54(9):52-62.

[9] Green, D. W., Gorman, T. M., Evans, J. W., and J. F. Murphy. 2006. Mechanical Grading of Round Timber Beams. *J. Mat. Civil Engineering*. 18(1):1-10.

[10] Green, D. W., Gorman, T. M., Evans, J. W., Murphy, J. F., and C. A. Hatfield. 2008. Grading and properties of small-diameter Douglas-fir and ponderosa pine tapered logs. *Forest Products Journal*. 58(11):33-41.

[11] Green, D. W., Gorman, T. M., Murphy, J. F., and M. B. Wheeler. 2007. Moisture Content and the Properties of Lodgepole Pine Logs in Bending and Compression Parallel to the Grain. Res. Paper FPL-RP-639. USDA Forest Serv., Forest Prod. Lab., Madison, WI. 11 pp.

[12] Kretschmann, D. E. and D. W. Green. 1999. Mechanical grading of oak timbers. *J. Mat. Civil Engineering*. 11(2):91-97.

[13] LeVon-Green, S. L. and J. M. Livingston. 2003. Uses for Small-Diameter and Low-Value Forest Thinnings. *Ecological Restoration*. 21(1):34-38.

[14] Livingston, J. M. 2004. Small-Diameter Success Stories. USDA Forest Serv., Forest Prod. Lab., Madison, WI. 33 pp.

[15] Pieterse, J. K. and J. W. Lewis. 2012. Non-linear least squares. http://www.jkp-ads.com/Download.asp. Accessed September 18, 2016.

[16] Timber Products Inspection, Inc. (TP). 2017. Log Program Technical Guide. TP, Conyers, GA. http://www.tpinspection.com/log-home-services.php. Accessed April 9, 2017.

[17] Wang, X., Ross, R. J., Mattson, J. A., Erickson, J. R., Forsman, J. W., Geske, E. A., and M. A. Wehr. 2001. Several nondestructive evaluation techniques for assessing stiffness and MOE of Small-Diameter Logs. Res. Paper FPL-RP-600. USDA Forest Serv., Forest Prod. Lab., Madison, WI. 12 pp.

Appendix

Appendix A: 4-inch, 8-foot logs, with matched sets where A and B were taken from the same log, third-point test data MOE (ksi), points of rotation are 45° apart [Bowers, C. L. 2012. *Use of a single, mid-span load to determine the MOE of small diameter structural logs*. Master's thesis. University of Idaho, Moscow.]

	Diameter	Point of Rotation							
Log ID	(in)	1	2	3	4	5	6	7	8
401A	3.88	1536.7	1590.1	1546.7	1444.0	1470.1	1585.6	1573.5	1485.1
401B	3.88	1432.0	1488.5	1439.7	1406.8	1395.1	1466.9	1395.1	1410.8
402A	3.9	1074.1	1061.3	1018.4	1039.5	1067.8	1033.9	1014.8	1056.6
402B	3.9	1173.9	1086.3	1081.7	1166.0	1220.7	1138.2	1091.0	1179.6
403A	3.88	1237.9	1247.9	1289.2	1287.9	1216.2	1239.3	1286.7	1251.3
403B	3.87	1178.9	1210.1	1239.7	1244.1	1183.4	1177.5	1207.3	1226.4
404A	3.9	1481.4	1556.5	1581.3	1524.1	1512.9	1570.5	1620.5	1517.8
404B	3.88	1497.3	1453.3	1486.6	1520.7	1490.6	1442.8	1504.3	1527.2
405A	3.9	1367.9	1307.9	1321.3	1383.2	1355.9	1315.1	1344.5	1381.6
405B	3.88	1287.8	1273.1	1219.1	1267.3	1299.5	1312.4	1216.9	1292.5
406A	3.86	1460.0	1501.1	1532.3	1455.8	1449.0	1475.8	1496.5	1446.1
406B	3.85	1497.4	1500.9	1443.8	1441.7	1491.7	1512.0	1466.6	1474.9
407A	3.87	1592.0	1554.1	1592.6	1570.1	1576.2	1590.4	1590.0	1557.0
407B	3.85	1569.5	1564.6	1559.4	1525.7	1517.2	1576.1	1617.1	1560.2
408A	3.87	1586.4	1643.9	1638.7	1628.0	1630.1	1692.7	1664.6	1663.8
408B	3.87	1530.8	1541.5	1551.6	1531.8	1552.6	1572.4	1577.7	1567.7
409A	3.89	1568.1	1610.0	1771.2	1667.2	1596.5	1595.5	1634.2	1643.6
409B	3.87	1807.8	1821.4	1829.8	1885.7	1828.9	1786.9	1797.3	1861.1
410A	3.86	1700.9	1685.8	1621.5	1661.0	1711.9	1632.5	1663.7	1682.9
410B	3.85	1589.8	1612.0	1662.2	1628.9	1601.6	1596.6	1658.0	1666.8
411A	3.82	1482.9	1491.0	1501.8	1493.3	1501.2	1510.6	1531.4	1464.9
411B	3.83	1466.0	1462.1	1430.2	1483.9	1510.1	1490.2	1488.0	1473.3
412A	3.87	1459.4	1528.4	1430.9	1380.3	1461.6	1531.2	1445.3	1397.2
412B	3.86	1415.4	1513.1	1349.6	1304.9	1428.2	1469.1	1407.2	1297.7
413A	3.88	1514.1	1474.2	1501.9	1540.6	1481.4	1471.1	1486.8	1514.8
413B	3.87	1422.3	1346.5	1411.4	1446.5	1418.6	1369.7	1421.0	1455.3
414A	3.9	1332.7	1292.2	1311.9	1391.2	1327.5	1236.8	1291.3	1365.1
414B	3.9	1367.0	1338.0	1351.9	1370.7	1358.0	1370.4	1389.6	1337.2
415A	3.87	1112.6	1081.0	1079.8	1106.0	1111.2	1098.9	1070.9	1068.8
415B	3.9	1017.7	1033.6	1072.8	1031.1	1049.4	1099.1	1058.6	1003.5

Appendix A (continued)

Log ID	Diameter (in)	Point of Rotation 1	2	3	4	5	6	7	8
416A	3.88	1640.5	1664.9	1568.8	1575.1	1624.8	1637.8	1613.1	1586.5
416B	3.89	1516.3	1526.7	1479.2	1416.2	1463.6	1537.7	1472.0	1459.5
417A	3.87	1251.2	1277.6	1281.9	1330.0	1278.4	1249.8	1299.0	1322.0
417B	3.86	1142.5	1128.8	1169.6	1163.4	1140.8	1141.6	1163.9	1162.1
418A	3.85	1712.5	1658.7	1717.2	1739.5	1723.1	1726.6	1703.0	1651.2
418B	3.87	1645.6	1617.7	1643.7	1650.7	1643.1	1615.3	1591.5	1608.0
419A	3.89	938.1	923.3	952.8	952.0	909.7	899.9	935.5	921.7
419B	3.88	987.9	1002.6	1054.1	1028.7	972.4	999.2	1059.7	1053.1
420A	3.87	1265.4	1184.5	1243.1	1264.7	1282.6	1215.4	1189.1	1287.3
420B	3.87	1241.6	1236.6	1247.4	1242.3	1251.9	1264.9	1252.5	1252.4
421A	3.9	902.9	854.8	910.6	951.9	890.3	847.6	876.9	961.8
421B	3.9	814.6	805.8	787.8	779.8	795.0	793.6	775.3	776.8
423A	3.87	1308.3	1281.0	1260.8	1286.0	1309.2	1284.3	1261.3	1300.7
423B	3.87	1427.8	1422.5	1376.5	1343.2	1454.4	1417.4	1308.5	1368.0
424A	3.88	1271.6	1253.8	1312.7	1336.7	1292.4	1271.9	1333.0	1357.6
424B	3.89	1312.8	1278.9	1285.1	1301.1	1272.0	1285.1	1269.5	1309.4
425A	3.89	1265.9	1277.9	1240.1	1256.9	1294.7	1314.0	1268.7	1263.4
425B	3.87	1343.3	1278.9	1233.5	1230.5	1287.2	1383.8	1262.5	1265.8
426A	3.9	1327.4	1243.6	1248.4	1279.6	1298.9	1246.4	1222.9	1278.5
426B	3.88	1413.5	1414.5	1393.3	1421.4	1395.6	1386.4	1353.8	1379.5
427A	3.88	1563.5	1528.5	1506.3	1522.0	1554.8	1517.1	1483.6	1534.6
427A	3.86	1649.6	1630.9	1670.6	1633.2	1631.9	1637.7	1655.3	1676.3
427B	3.88	1442.2	1483.5	1478.8	1449.9	1441.7	1434.8	1447.3	1422.8
427B	3.89	1465.1	1453.0	1441.4	1445.7	1453.8	1475.5	1438.0	1443.8
428A	3.9	1330.5	1358.8	1358.1	1321.8	1321.8	1340.9	1379.6	1357.4
428B	3.89	1343.1	1298.0	1338.4	1368.9	1323.5	1279.4	1339.9	1379.3
429A	3.89	1576.7	1556.4	1558.1	1539.0	1581.9	1566.7	1537.0	1520.4
429B	3.89	1582.5	1586.9	1563.2	1504.3	1575.3	1604.4	1554.6	1531.5
430A	3.88	1556.6	1612.8	1630.6	1601.5	1597.2	1624.1	1617.6	1610.3
430B	3.88	1465.1	1544.0	1556.0	1522.3	1484.0	1516.2	1491.5	1449.0

Appendix B: 6-inch 12 foot logs third-point test data MOE (ksi), points of rotation are 450 apart [Bowers, C. L. 2012. *Use of a single, mid-span load to determine the MOE of small diameter structural logs*. Master's thesis. University of Idaho, Moscow.]

	Diameter	Point of Rotation							
Log ID	(in)	1	2	3	4	5	6	7	8
601	5.84	1627.8	1583.0	1591.4	1628.2	1641.5	1596.9	1566.8	1629.1
602	5.8	1891.9	1860.1	1942.3	1929.3	1880.3	1865.1	1902.2	1925.5
603	5.82	1839.0	1851.1	1832.5	1781.9	1779.6	1808.4	1826.8	1780.6
604	5.79	1865.1	1923.1	1894.3	1905.7	1818.7	1865.4	1910.5	1895.0
605	5.81	1877.9	1846.8	1876.0	1848.2	1829.9	1830.0	1867.0	1843.6
606	5.82	1944.3	1928.0	1833.2	1818.7	1922.3	1935.1	1889.4	1784.0
607	5.8	2098.3	1996.7	1963.3	2024.8	2081.3	2026.0	2061.6	1994.2
608	5.84	1908.9	1909.1	1923.4	1911.3	1876.6	1967.4	1930.1	1918.3
609	5.87	1452.3	1444.5	1447.2	1367.2	1357.3	1456.9	1432.6	1365.3
610	5.85	1702.6	1737.7	1741.1	1694.4	1640.8	1720.0	1733.4	1697.9
611	5.82	2229.7	2162.8	2155.2	2197.9	2200.5	2171.3	2106.0	2083.6
612	5.85	1677.3	1645.9	1689.3	1703.1	1677.3	1667.3	1697.0	1707.8
613	5.81	1603.4	1625.8	1698.0	1681.0	1633.5	1605.1	1613.9	1654.8
614	5.85	1602.3	1573.6	1574.7	1576.3	1610.4	1555.7	1595.8	1535.3
615	5.78	2148.2	2123.4	2110.0	2098.0	2153.0	2218.3	2188.8	2093.8
616	5.83	1972.0	1961.2	1922.3	1977.3	1989.5	2018.8	1978.4	1931.1
617	5.9	1050.5	1034.7	1037.6	1030.5	1017.2	1074.2	1064.7	1036.9
618	5.84	1419.5	1412.5	1384.6	1408.1	1396.5	1380.6	1341.5	1374.9
619	5.8	1948.6	1964.2	1976.9	1931.0	1875.5	1935.2	1967.0	1968.0
620	5.83	1555.1	1525.5	1523.9	1573.8	1577.3	1547.1	1583.7	1561.4
621	5.82	2172.6	2083.2	2121.0	2176.4	2140.3	2112.0	2053.6	2130.1
622	5.85	1228.5	1192.9	1159.2	1221.9	1260.5	1242.6	1174.4	1187.6
623	5.86	1504.4	1560.6	1474.7	1468.3	1484.1	1603.2	1524.6	1502.3
624	5.85	1422.0	1371.8	1375.8	1387.5	1395.2	1346.9	1353.3	1392.4
625	5.84	1717.1	1723.4	1687.9	1692.6	1726.3	1695.8	1656.6	1700.4
626	5.78	2278.4	2242.7	2224.8	2285.0	2219.4	2286.3	2213.1	2209.5
627	5.78	1995.6	2029.3	2013.4	1968.7	1964.4	1992.0	2029.1	1980.8
628	5.82	1620.2	1584.6	1776.3	1669.3	1524.7	1573.9	1802.9	1771.6
629	5.85	1375.2	1453.5	1440.9	1420.8	1381.4	1411.1	1434.1	1382.6
630	5.85	1353.1	1367.7	1343.8	1338.5	1380.2	1360.1	1316.0	1292.4

Appendix C: Log ID, MC %, Length, Diameter, Density, SWV, Third-point MOE, Mid-point MOE, Dynamic MOE and Grade

Species	Log ID	MC (%)	Length (in.)	Diameter of Log (in.)	Density (lb/ft^3)	Stress-Wave Velocity (fps)	MOE (Third-point) (psi)	MOE (Mid-Point) (psi)	MOE (Dynamic) (psi)	TPI Log Grade
Larch	La-1-0	18	150	5.9	37.0	16568	2.41E+06	1.81E+06	2.19E+06	Unsawn Round
	La-1-90						2.42E+06	1.98E+06		
	La-2-0	18	151	5.9	39.6	17224	2.72E+06	2.05E+06	2.54E+06	Unsawn Round
	La-2-90						2.79E+06	2.23E+06		
	La-3-0	21	149	5.9	36.7	15420	2.04E+06	1.40E+06	1.88E+06	Unsawn Round
	La-3-90						1.91E+06	1.42E+06		
	La-4-0	23	150	5.9	37.6	15453	2.17E+06	1.53E+06	1.94E+06	Unsawn Round
	La-4-90						2.16E+06	1.54E+06		
	La-5-0	18	150	5.9	37.1	15715	2.23E+06	1.54E+06	1.98E+06	Unsawn Round
	La-5-90						2.13E+06	1.48E+06		
	La-6-0	19	149	5.9	37.9	17060	2.58E+06	1.85E+06	2.38E+06	Unsawn Round
	La-6-90						2.66E+06	1.78E+06		
	La-7-0	20	150	5.9	36.1	14928	1.95E+06	1.44E+06	1.74E+06	Unsawn Round
	La-7-90						1.94E+06	1.42E+06		
	La-8-0	21	148	5.9	41.3	17224	2.85E+06	1.94E+06	2.64E+06	Unsawn Round
	La-8-90						2.56E+06	1.98E+06		
	La-9-0	22	151	6.0	35.1	14567	1.81E+06	1.28E+06	1.61E+06	Unsawn Round
	La-9-90						1.76E+06	1.27E+06		
	La-10-0	9	94	3.9	29.8	12992	1.13E+06	9.40E+05	1.09E+06	No. 1
	La-10-90						1.13E+06	1.04E+06		

Appendix C (continued)

Species	Log ID	MC (%)	Length (in.)	Diameter of Log (in.)	Density (lb/ft^3)	Stress-Wave Velocity (fps)	MOE (Third-point) (psi)	MOE (Mid-Point) (psi)	MOE (Dynamic) (psi)	TPI Log Grade
Lodgepole pine	LP-1-0	15	145	5.9	29.6	14042	1.40E+06	9.76E+05	1.26E+06	Cull
	LP-1-90						1.28E+06	8.70E+05		
	LP-2-0	17	145	5.9	32.2	13353	1.61E+06	1.18E+06	1.24E+06	Cull
	LP-2-90						1.58E+06	1.10E+06		
	LP-3-0	19	146	5.9	28.9	12762	1.13E+06	7.92E+05	1.01E+06	Cull
	LP-3-90						1.20E+06	9.63E+05		
	LP-4-0	16	145	5.9	32.9	13944	1.70E+06	1.42E+06	1.38E+06	Unsawn Round
	LP-4-90						1.41E+06	1.30E+06		
	LP-5-0	14	146	5.9	27.0	13911	1.47E+06	1.02E+06	1.13E+06	No. 3
	LP-5-90						1.45E+06	1.05E+06		
	LP-6-0	13	146	5.9	28.3	13353	1.42E+06	1.02E+06	1.09E+06	Cull
	LP-6-90						1.41E+06	1.01E+06		
	LP-7-0	19	146	5.9	30.8	12303	1.21E+06	9.19E+05	1.01E+06	Cull
	LP-7-90						1.19E+06	9.47E+05		
	LP-8-0	20	145	5.9	32.0	13780	1.66E+06	1.21E+06	1.31E+06	Unsawn Round
	LP-8-90						1.58E+06	1.06E+06		
	LP-9-0	17	146	5.9	32.8	14501	1.76E+06	1.23E+06	1.49E+06	Unsawn Round
	LP-9-90						1.74E+06	1.27E+06		
	LP-10-0	17	146	5.9	28.1	13747	1.44E+06	9.99E+05	1.15E+06	No. 3
	LP-10-90						1.38E+06	9.40E+05		

Appendix C (continued)

Species	Log ID	MC (%)	Length (in.)	Diameter of Log (in.)	Density (lb/ft^3)	Stress-Wave Velocity (fps)	MOE (Third-point) (psi)	MOE (Mid-Point) (psi)	MOE (Dynamic) (psi)	TPI Log Grade
Ponderosa pine	PP-1-0	8	100	3.9	21.7	11024	6.47E+05	5.06E+05	5.68E+05	Cull
	PP-1-90						6.21E+05	5.01E+05		
	PP-2-0	11	94	3.9	29.8	8034	4.56E+05	3.46E+05	4.15E+05	Cull
	PP-2-90						3.96E+05	2.14E+05		
	PP-3-0	10	101	3.9	26.2	11516	8.09E+05	6.90E+05	7.50E+05	Cull
	PP-3-90						7.97E+05	5.82E+05		
	PP-4-0	7	95	3.9	26.8	9318	6.13E+05	4.92E+05	5.02E+05	Cull
	PP-4-90						6.42E+05	N/A		
	PP-5-0	9	100	3.9	25.4	8169	4.02E+05	3.13E+05	3.65E+05	Cull
	PP-5-90						3.77E+05	1.93E+05		
	PP-6-0	11	103	3.9	25.1	12598	9.56E+05	7.92E+05	8.59E+05	Cull
	PP-6-90						9.20E+05	7.64E+05		
	PP-7-0	9	101	3.9	29.0	10203	8.42E+05	7.05E+05	6.52E+05	Cull
	PP-7-90						8.20E+05	6.56E+05		
	PP-8-0	10	101	3.9	24.1	12008	8.90E+05	7.23E+05	7.52E+05	Cull
	PP-8-90						8.16E+05	6.66E+05		
	PP-9-0	12	101	3.9	24.4	11909	8.16E+05	6.25E+05	7.46E+05	Cull
	PP-9-90						8.35E+05	6.62E+05		
	PP-10-0	10	102	3.9	22.9	11877	8.10E+05	6.15E+05	6.98E+05	Cull
	PP-10-90						7.45E+05	6.02E+05		

Appendix C (continued)

Species	Log ID	MC (%)	Length (in.)	Diameter of Log (in.)	Density (lb/ft^3)	Stress-Wave Velocity (fps)	MOE (Third-point) (psi)	MOE (Mid-Point) (psi)	MOE (Dynamic) (psi)	TPI Log Grade
Douglas-fir	Df-1-0	10	109	3.9	31.0	14567	1.39E+06	1.12E+06	1.42E+06	Unsawn Round
	Df-1-90						1.40E+06	1.29E+06		
	Df-2-0	11	109	3.9	32.4	16535	2.06E+06	1.53E+06	1.91E+06	Unsawn Round
	Df-2-90						2.07E+06	1.56E+06		
	Df-3-0	10	107	3.9	31.3	15289	1.61E+06	1.34E+06	1.58E+06	Unsawn Round
	Df-3-90						1.53E+06	1.39E+06		
	Df-4-0	11	108	3.9	35.7	17224	2.28E+06	1.70E+06	2.28E+06	Unsawn Round
	Df-4-90						2.30E+06	1.97E+06		
	Df-5-0	10	96	3.9	30.4	15453	1.60E+06	1.40E+06	1.57E+06	Unsawn Round
	Df-5-90						1.64E+06	1.15E+06		
	Df-6-0	9	112	3.9	29.6	14862	1.44E+06	1.22E+06	1.41E+06	Unsawn Round
	Df-6-90						1.42E+06	1.22E+06		
	Df-7-0	10	109	3.9	31.8	16109	1.67E+06	1.26E+06	1.78E+06	Unsawn Round
	Df-7-90						1.84E+06	1.52E+06		
	Df-8-0	10	110	3.9	36.4	13287	1.34E+06	1.23E+06	1.39E+06	No. 3
	Df-8-90						1.40E+06	1.04E+06		
	Df-9-0	11	107	3.9	30.7	15617	1.70E+06	1.37E+06	1.62E+06	Unsawn Round
	Df-9-90						1.75E+06	1.48E+06		
	Df-10-0	11	110	3.9	36.1	17881	2.49E+06	2.06E+06	2.49E+06	Unsawn Round
	Df-10-90						2.58E+06	2.15E+06		

Appendix C (continued)

Species	Log ID	MC (%)	Length (in.)	Diameter of Log (in.)	Density (lb/ft^3)	Stress-Wave Velocity (fps)	MOE (Third-point) (psi)	MOE (Mid-Point) (psi)	MOE (Dynamic) (psi)	TPI Log Grade
Grand fir	GF-1-0	9	107	3.9	24.5	15617	1.18E+06	9.46E+05	1.29E+06	No. 2
	GF-1-90						1.26E+06	1.06E+06		
	GF-2-0	11	107	3.9	24.8	16896	1.57E+06	1.31E+06	1.53E+06	Unsawn Round
	GF-2-90						1.51E+06	1.30E+06		
	GF-3-0	10	106	3.9	24.5	17552	1.62E+06	1.35E+06	1.63E+06	Unsawn Round
	GF-3-90						1.64E+06	1.39E+06		
	GF-4-0	9	110	3.9	21.2	14337	1.09E+06	8.77E+05	9.41E+05	No. 2
	GF-4-90						1.03E+06	7.85E+05		
	GF-5-0	10	108	3.9	25.8	17552	1.72E+06	1.45E+06	1.72E+06	Unsawn Round
	GF-5-90						1.80E+06	1.38E+06		
	GF-6-0	11	110	3.9	25.8	14009	1.24E+06	1.01E+06	1.09E+06	Unsawn Round
	GF-6-90						1.21E+06	1.04E+06		
	GF-7-0	13	110	3.9	27.8	17717	1.92E+06	1.64E+06	1.89E+06	Unsawn Round
	GF-7-90						1.83E+06	1.67E+06		
	GF-8-0	12	110	3.9	27.9	15453	1.56E+06	1.24E+06	1.44E+06	No. 2
	GF-8-90						1.48E+06	1.21E+06		
	GF-9-0	11	110	3.9	28.3	16339	1.63E+06	1.51E+06	1.63E+06	No. 2
	GF-9-90						1.67E+06	1.36E+06		
	GF-10-0	10	111	3.9	23.3	18045	1.55E+06	1.48E+06	1.64E+06	Cull
	GF-10-90						1.67E+06	1.38E+06		

Appendix D: Sine Wave Data (Log Number, Amplitude, Mean, Offset and ANOVA result)

Log Number	**Amplitude (ksi)**	**Upper or Lower Limit (ksi)**	**Offset (°)**	**ANOVA**
1	167.89	1420	-210.5	0.0105
2	68.59	1385	-214.0	0.2630
3	-53.24	1079	-184.4	0.0370
4	-159.33	1246	-196.6	0.0088
5	-81.12	1310	-255.8	0.0157
6	-77.43	1259	-245.3	0.0474
7	136.35	1457	-194.9	0.0079
8	76.33	1444	-137.0	0.0007
9	93.27	1287	-121.0	0.0017
10	86.71	1218	-86.9	0.0154
11	90.06	1418	-20.4	0.0354
12	80.81	1426	-66.9	0.0210
13	15.81	1568	-44.2	0.6713
14	66.86	1518	-19.7	0.2786
15	62.39	1604	-9.3	0.2499
16	28.37	1535	-11.9	0.4915
17	160.89	1531	15.9	0.1092
18	69.95	1783	55.2	0.1925
19	72.18	1624	78.9	0.1476
20	99.92	1562	18.9	0.0074
21	42.86	1469	-26.5	0.2655
22	-29.96	1494	-7.8	0.6046
23	-156.56	1553	37.9	0.0002
24	-220.45	1539	34.7	0.0046
25	-56.99	1533	-40.9	0.0349
26	-93.07	1470	-38.2	0.0247
27	-134.58	1404	-35.1	0.0085
28	7.44	1355	27.5	0.9623
29	-38.22	1115	3.5	0.0976
30	-75.12	1095	64.9	0.1772

Appendix D (continued)

Log Number	**Amplitude (ksi)**	**Upper or Lower Limit (ksi)**	**Offset (°)**	**ANOVA**
31	-104.27	1682	28.3	0.0149
32	-103.89	1550	37.4	0.0282
33	-82.97	1339	-55.9	0.0138
34	-48.63	1183	-68.2	0.0033
35	5.20	1701	-45.0	0.9899
36	-37.23	1651	-12.1	0.4199
37	-42.04	957	111.1	0.2652
38	-108.46	1090	106.5	0.0016
39	-123.82	1322	155.6	0.0226
40	6.13	1245	158.7	0.9012
41	-106.46	965	137.7	0.0019
42	-41.28	818	200.1	0.0381
43	-55.15	1322	169.3	0.0054
44	-150.96	1488	197.8	0.0133
45	116.45	1228	209.2	0.0038
46	-35.78	1312	149.4	0.2409
47	-57.35	1310	208.7	0.1294
48	-139.12	1376	205.6	0.1106
49	-104.54	1336	167.2	0.0026
50	-29.58	1414	171.3	0.5744
51	-67.32	1568	174.4	0.0071
52	39.41	1622	204.5	0.2684
53	-40.59	1477	248.5	0.3872
54	-36.29	1476	204.5	0.0586
55	-50.22	1378	260.6	0.0789
56	-87.84	1389	308.8	0.0092
57	59.00	1516	297.2	0.0588
58	92.99	1504	306.3	0.0018
59	57.09	1570	352.2	0.0435
60	86.61	1447	340.1	0.2243

Appendix D (continued)

Log Number	**Amplitude (ksi)**	**Upper or Lower Limit (ksi)**	**Offset (°)**	**ANOVA**
61	-82.47	1373	351.3	0.0039
62	73.76	1642	378.4	0.2501
63	65.15	1559	433.7	0.0534
64	-28.36	1678	433.9	0.3837
65	52.17	1637	183.1	0.0393
66	-127.43	1670	376.1	0.0294
67	-67.49	1805	359.5	0.0004
68	13.39	1644	348.7	0.8912
69	148.56	1234	327.1	0.0027
70	87.76	1452	328.9	0.0389
71	179.82	1681	288.6	0.0189
72	-58.01	1482	287.5	0.0775
73	49.27	1457	238.8	0.0344
74	-9.68	1457	326.1	0.7764
75	45.57	1769	309.0	0.0323
76	-85.69	1721	346.8	0.0020
77	-24.16	963	248.1	0.2084
78	94.43	1240	262.1	0.0056
79	-45.14	1764	152.2	0.2714
80	-46.89	1413	135.0	0.0458
81	69.54	1704	221.9	0.0087
82	-68.83	1087	366.0	0.0038
83	76.48	1390	328.5	0.0188
84	70.80	1199	79.6	0.0210
85	-42.64	1506	199.8	0.0098
86	-53.44	1924	215.8	0.0325
87	-43.74	1789	268.7	0.0073
88	-269.41	1669	294.9	0.0005
89	63.31	1227	345.8	0.0022
90	-73.14	1304	195.4	0.0024

Appendix E: Example of ANOVA results and graph (Log Number 90)

x	y	yhat	(y - yhat)²		Constants	Initial guesses, final solver results.
0	1287	1285	7		Const_a	-73.14451285
45	1278	1268	100		Const_b	1304.196182
90	1229	1234	18		Const_c	195.3783777
135	1234	1241	39			
180	1283	1285	5			
225	1258	1268	108			
270	1239	1234	27			
315	1246	1241	28			
					SS	332.9370425
Equation:		y = A (ABS(sin (x-C)) + B				

Source	Degrees of Freedom	Sum of squares	Mean Square	F	P value
Model	2	3414.784	1707.392	25.623	0.002
Error	5	333.182	66.636		
Total	7	3747.965